Computer Methods and Programs in Biomedicine 220 (2022) 106819

Contents lists available at ScienceDirect

Computer Methods and Programs in Biomedicine

journal homepage: www.elsevier.com/locate/cmpb

Physiological trend analysis of a novel cardio-pulmonary model during a preload reduction manoeuvre

James Cushway[a,*], Liam Murphy[a], J. Geoffrey Chase[a], Geoffrey M. Shaw[b], Thomas Desaive[c]

[a] University of Canterbury, Department of Mechanical Engineering, Christchurch, New Zealand
[b] Dept of Intensive Care, Christchurch Hospital, Christchurch, New Zealand
[c] University of Liège (ULg), GIGA-Cardiovascular Sciences, Liège, Belgium

ARTICLE INFO

Article history:
Received 2 February 2022
Revised 13 April 2022
Accepted 14 April 2022

Keywords:
Positive end-expiratory pressure
Stressed blood volume
Cardiovascular
Cardio-pulmonary
Thoracic pressure

ABSTRACT

Background and objective: Mechanical ventilation causes adverse effects on the cardiovascular system. However, the exact nature of the effects on haemodynamic parameters is not fully understood. A recently developed cardio-vascular system model which incorporates cardio-pulmonary interactions is compared to the original 3-chamber cardiovascular model to investigate the exact effects of mechanical ventilation on haemodynamic parameters and to assess the trade-off of model complexity and model reliability between the 2 models.

Methods: Both the cardio-pulmonary and three chamber models are used to identify cardiovascular system parameters from aortic pressure, left ventricular volume, airway flow and airway pressure measurements from 4 pigs during a preload reduction manoeuvre. Outputs and parameter estimations from both models are contrasted to assess the relative performance of each model and to further investigate the effects of mechanical ventilation on haemodynamic parameters.

Results: Both models tracked measurements accurately as expected. There was no identifiable increase in error from the added complexity of the cardio-pulmonary model, with both models having a mean average error below 0.5% for all pigs. Identified left ventricle and vena cava elastances of the 3-chamber model was found to diverge exponentially with PEEP from identified left ventricle and vena cava elastances of the cardio-pulmonary model. The r^2 of the fit for each pig ranged from 0.888 to 0.998 for left ventricle elastance divergence and from 0.905 to 0.999 for vena cava elastance divergence. All other identified parameters showed no significant difference between models.

Conclusions: Despite the increase in model complexity, there was no loss in the cardio-pulmonary model's ability to accurately estimate haemodynamic parameters and reproduce system dynamics. Furthermore, the cardio-pulmonary model was able to demonstrate how mechanical ventilation affected parameter estimations as PEEP was increased. The 3-chamber model was shown to produce parameter estimations which diverged exponentially with PEEP, while the cardiopulmonary model estimations remained more stable, suggesting its ability to produce more physiologically accurate parameter estimations under higher PEEP conditions.

1. Introduction

Mechanical ventilation is a critical support for many patients in ICU. Positive-end expiratory pressure (PEEP) is used to maximise alveoli recruitment for increased blood oxygenation. However, excessive PEEP is dangerous and can cause lung damage [1]. Elevated levels of PEEP also cause an increase of pressure in the thoracic chamber, where the heart and vena cava are located. This rise in intra-thoracic pressure (ITP) is known to decrease cardiac preload, and thus, decrease venous return, ultimately reducing both the stroke volume (SV) and stressed blood volume (SBV) of the system [2–4].

SBV is defined as the total pressure-generating blood volume in the circulation and describes the volume contributing to tissue perfusion. Recently, SBV has been shown to be a potential index of fluid responsiveness as it is a major determinant of the mean systemic filling pressure (MSFP) and thus, venous return, making

* Corresponding author.
E-mail address: james.cushway@pg.canterbury.ac.nz (J. Cushway).

https://doi.org/10.1016/j.cmpb.2022.106819
0169-2607/

it a potentially important diagnostic tool [5]. However, clinically determining the SBV of a patient is a highly complex and dangerous procedure, involving multiple cardiac arrests and fluid infusions, and is clearly not a clinically viable diagnostic procedure [6]. Therefore, accurate model based or other surrogates are required if SBV is to be used as an index of fluid responsiveness.

Several lumped parameter models have been presented, most commonly the 6 and 3-chamber models [7–11], as reviewed in [12]. While simple, identifiable models have proven successful at capturing the fundamental system dynamics of the CVS and estimation of total SBV. However, they do not typically include the pulmonary system or the impact of ventilation. Instead they rely on the effects of the pulmonary system to be contained in the left ventricle and vena cava pressure waveforms. Given the complex relationship mechanical ventilation has on the CVS, the ability to directly account for its effects could prove important in reliable patient state estimation and in using SBV as an index of fluid resuscitation.

De Bournonville et al. [13] presented a cardio-pulmonary model combining 2 separate, clinically validated models of the cardiovascular and respiratory systems. The model reproduced the effects of mechanical ventilation on the CVS. However, while the study demonstrated the impact of PEEP on haemodynamic parameters, it did not demonstrate whether the added model complexity significantly improved the simulation of cardiovascular measurements. In particular, the parameter estimation process and identifiability were not addressed, so there is no assessment of the impact of the combined model on the value and trends of haemodynamic parameters as PEEP and other MV settings change. Thus, its identifiability and clinical utility are unknown, particularly in contrast to the simpler original, uncoupled, but clinically validated, 3-chamber cardiovascular model alone.

While model-based decision support is an emerging field [10], cardiovascular decision support for fluid administration to improve SBV and avoid excessive fluid administration is an important clinical area which has not been well-studied [12]. Excessive fluid administration also significantly impacts lung mechanics and function, and thus mechanical ventilation. The inter-relationship between cardiovascular system management and pulmonary system management is thus stronger, and both need to be accounted for in any decision support so their model-based management can be jointly achieved and optimised. This paper directly examines these clinically driven modelling interactions.

This study uses a 3-chamber minimal CVS model and a combined cardio-pulmonary model with cardiovascular measurements from a preload reduction manoeuvre (RM) performed on 4 pigs to address these issues and delineate the impact on model performance and parameter identification. The study also integrates a new driver function developed by Davidson et al. [14] to remove the need for left ventricular pressure measurements which are not usually available in a clinical setting.

2. Methods

2.1. Cardiovascular system model

The CVS model is a highly simplified lumped parameter model comprising of three chambers representing the left ventricle, aorta and vena cava. The chambers are connected by 3 flow resistances, which represent the output, input, and systemic resistance (R_o, R_i & R_c). The input and output valves of the ventricle chamber are represented by diodes, which prevent flow for a negative pressure gradient. This simple model ensures theoretical identifiability and maximises practical identifiability [15], which elude more complex and detailed models [12,16]. The model schematic is shown in Fig. 1.

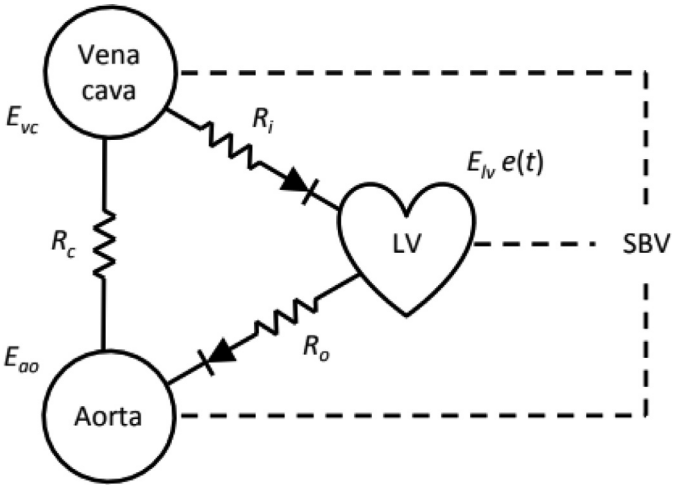

Fig. 1. Three chamber CVS model.

The chambers representing the aorta and vena cava are passive chambers [9], their pressures are thus defined:

$$P_a(t) = E_a(t)V_{s,a}(t), \tag{1}$$

$$P_{vc}(t) = E_{vc}(t)V_{s,vc}(t), \tag{2}$$

Where P_{ao} and P_{vc} represent aortic and venous pressure, $V_{s,ao}$ and $V_{s,vc}$ represent the stressed volume of the aorta and vena cava, and E_{ao} and E_{vc} represent aortic and venous elastance.

The left ventricle contracts during each heartbeat making it an active chamber. Left ventricle pressure is thus defined using time varying elastance as a driver function [7]:

$$P_{lv}(t) = e(t)E_{lv}V_{s,lv}(t) \tag{3}$$

where $e(t)$ is the driver function of the left ventricle derived from Davidson et al. [14].

The flow into each of the chambers is modelled using Ohm's law. The systemic flow is thus defined:

$$Q_c(t) = \frac{P_a(t) - P_{vc}(t)}{R_c}. \tag{4}$$

The input and output flows to the left ventricle are controlled by valves preventing flow across a negative pressure gradient. These flows can be represented using piecewise functions:

$$Q_o(t) = \begin{cases} \frac{P_{lv}(t) - P_{ao}(t)}{R_o} & P_{lv}(t) > P_{ao}(t) \\ 0 & \text{else} \end{cases} \tag{5}$$

$$Q_i(t) = \begin{cases} \frac{P_{vc}(t) - P_{lv}(t)}{R_i} & P_{vc}(t) > P_{lv}(t) \\ 0 & \text{else.} \end{cases} \tag{6}$$

The rate of change of stressed volume for each chamber is given by the difference of input and output flow:

$$\dot{V}_{s,ao}(t) = Q_o(t) - Q_c(t) \tag{7}$$

$$\dot{V}_{s,vc}(t) = Q_c(t) - Q_i(t) \tag{8}$$

$$\dot{V}_{s,lv}(t) = Q_i(t) - Q_o(t) \tag{9}$$

The CVS is a closed system and its total rate of change of volume is zero, yielding:

$$\dot{V}_{s,lv}(t) + \dot{V}_{s,a}(t) + \dot{V}_{s,vs}(t) = 0 \tag{10}$$

Integrating Eq. (10) gives the constant stressed blood volume for the system, $V_{s,3}$:

$$V_{s,3} = V_{s,lv} + V_{s,a} + V_{s,vc} \tag{11}$$

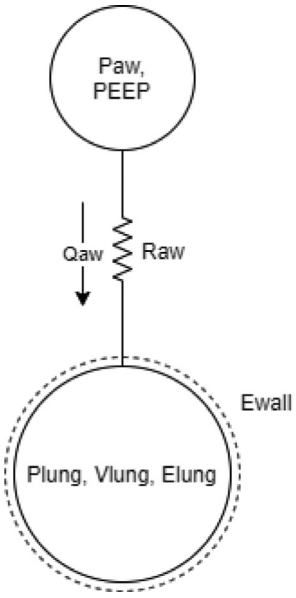

Fig. 2. Single chamber RS model.

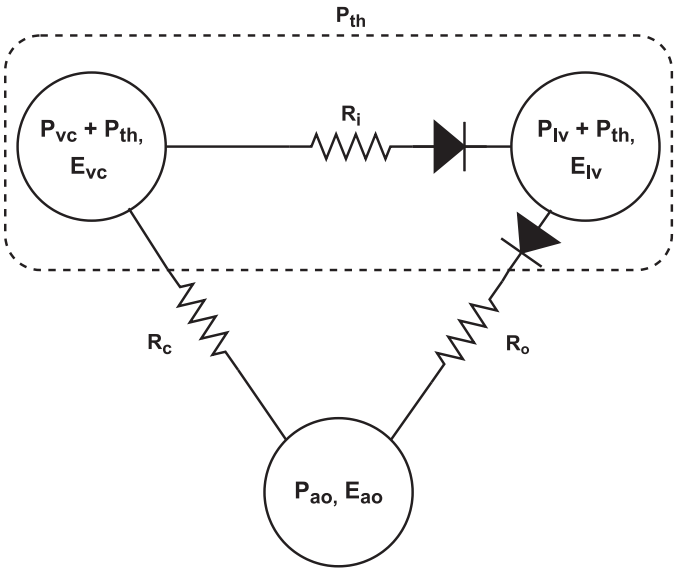

Fig. 3. Coupled cardiopulmonary model. The thoracic cavity is represented by the dashed line and exerts intra-thoracic pressure, P_{th}, on the vena cava and left ventricle.

The model is thus made up of a total of 7 parameters; 3 elastances (E_a, E_{lv}, E_{vc}), 3 resistances (R_c, R_i, R_o) and the total stressed blood volume of the system, $V_{s,3}$.

2.2. Respiratory system model

The respiratory system model is a clinically validated lumped parameter model made up of a single chamber to represent the lungs connected to a mechanical ventilator [1,17–22], as shown in Fig. 2. Airway flow is represented using Ohm's law:

$$Q_{aw}(t) = \frac{P_{aw}(t) - P_{lung}(t)}{R_{aw}}, \tag{12}$$

where P_{aw} is the airway pressure supplied by the ventilator, P_{lung} is the lung pressure and R_{aw} is the airway resistance. The lung is represented as a passive chamber, and the lung pressure can thus be defined:

$$P_{lung}(t) = E_{rs}V_{lung}(t) + PEEP \tag{13}$$

where V_{lung} is the lung air volume and E_{rs} is the respiratory system elastance. Lung volume is determined by integrating airway flow:

$$V_{lung}(t) = \int Q_{aw}(t)dt + \frac{PEEP}{E_{rs}} \tag{14}$$

Airway flow and pressure, and lung volume are provided by the ventilator. Substituting Eq. (13) into Eq. (12) yields airway pressure:

$$P_{aw}(t) = R_{aw}Q_{aw}(t) + E_{rs}V_{lung}(t) + PEEP \tag{15}$$

Linear regression can identify the parameters R_{aw} and E_{rs} from measured ventilator data.

2.3. Model coupling

The model coupling in this work is based on [13]. The CVS and RS models are coupled by thoracic pressure, the pressure exerted within the thoracic cavity due to the expansion of the lungs during mechanical ventilation [2–4]. The model schematic is shown in Fig. 3.

Thoracic pressure (P_{th}) is calculated from the respiratory system model:

$$P_{th}(t) = E_{wall}V_{lung}(t) \tag{16}$$

Table 1
Parameter Summary.

Parameter	Parameter Description
E_a	Aortic elastance
E_{lv}	Left ventricle elastance
E_{vc}	Vena cava elastance
R_c	Systemic resistance
R_i	Input resistance
R_o	Output resistance
$V_{s,3}$	Total stressed blood volume
E_{wall}	Chest wall elastance

where the wall elastance $E_{wall} = E_{rs} - E_{lung}$. Substituting Eq. (14) into Eq. (16), thoracic pressure can be expressed:

$$P_{th}(t) = E_{wall}V_c(t) + PEEP\frac{E_{wall}}{E_{rs}} \tag{17}$$

where $P_{th}(t)$ is the thoracic pressure and $V_c(t)$ is the tidal volume, $\int Q_{aw}(t)dt$.

The left ventricle and vena cava are located within the thoracic cavity and are directly influenced by ITP. However, the aorta is not located within the thoracic cavity and is not directly exposed. Therefore, the CVS model equations for venous and left ventricle pressure are updated:

$$P_{vc} = E_{vc}V_{s,vc}(t) + P_{th}(t) \tag{18}$$

$$P_{lv}(t) = e(t)E_{lv}V_{s,lv}(t) + P_{th}(t) \tag{19}$$

The final cardio-pulmonary model has a total of 8 parameters to identify, as summarised in Table 1.

2.4. Driver function model

Using the time varying elastance from Eq. (3), the driver function of the left ventricle can be defined:

$$e(t) = \frac{P_{lv}(t)}{V_{lv}(t) - V_u} \tag{20}$$

where V_u is the unstressed volume in the left ventricle. The driver function is used to drive the cardio-pulmonary model and contains crucial information pertaining to the cardiac cycle. However, measurements of left ventricle pressure and volume are not available

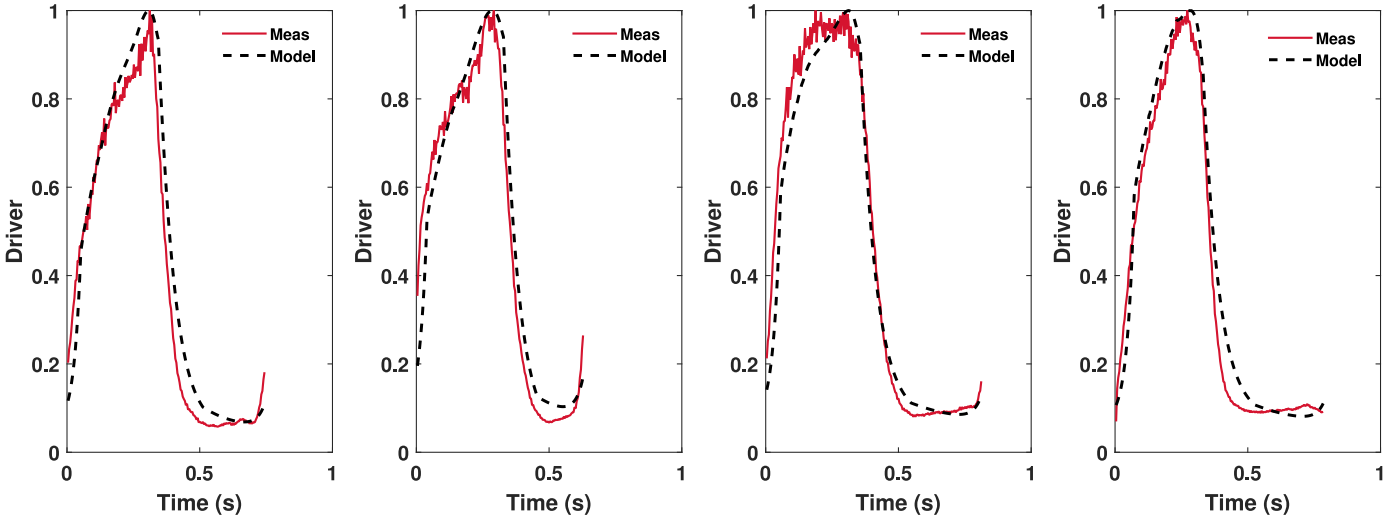

Fig. 4. Measured and modelled driver functions for each pig. From left to right, the plots represent the driver function of Pig 4, 6, 7 and 8 respectively.

in the ICU, as they are highly invasive. Thus, a modelled equivalent based on the work of Davidson et al. [14] is employed. This model recreates the pressure and volume waveforms from other available clinical measurements and simple physiological assumptions.

To reconstruct the left ventricle pressure waveform, it is assumed that aortic valve resistance is negligible, implying $P_{lv} = P_a$ during systole with some small amount of phase lag. During diastole, no information about P_{lv} can be extrapolated from P_a. However, the left ventricle is largely passive during diastole. Thus, the relaxation and filling phases can be modelled as an exponential decay and an exponential increase, respectively.

The V_{lv} waveform is reconstructed using piecewise phase-shifted sine waveforms in conjunction with 3 timings from the aortic pressure wave. Three pieces of volume information are also used: unstressed volume, end-systolic volume and end-diastolic volumes (V_d, V_{es}, & V_{ed}). For this study, unstressed volume was assumed to be 48% of V_{ed}. The V_{lv} and P_{lv} waveforms were recreated using the model from [14]. Finally, the driver function was calculated using Eq. (20). Figure 4 shows simulated and measured driver functions for each pig.

2.5. Output vector

Model outputs were chosen as beat-to-beat metrics, rather than time dependent measurements. This choice is largely due to the fact the temporal evolution of all signals is not always available or exportable from bedside machines [7]. As such, only beat-to-beat data, such as mean pressures and pulse pressures, are assumed to be available.

Outputs were chosen to ensure structural identifiablility of the model [15,23–25]. The work by Pironet gives lists of model outputs required to ensure structural identifiablility of the CVS model [7,10]. The output vector in Pironet's work is defined:

$$X_{cvs} = [\overline{P}_a(t),\ \Delta P_a(t),\ \overline{P}_{vc}(t),\ \Delta P_{vc}(t),\ \overline{V}_h(t),\ SV] \tag{21}$$

The pressure gradient between the left atrium and left ventricle determines the flow into the ventricle during filling. However, in the experiments performed, there were no measurements of left atrial pressure. Pironet's work used central venous pressure (CVP) as a reference measurement in place of left atrial pressure. However, in between CVP and left ventricle pressure lies the pulmonary circulation, and while CVP may be a close approximation, it is not necessarily a physiologically accurate one. Indeed, CVP was often found to be lower than $P_{lv}(t)$ during all of diastole, which would prevent ventricle filling. Therefore, due to the absence of left atrial pressure measurements and the unreliability of CVP as a reference, $\overline{P}_{vc}(t)$ and $\Delta P_{vc}(t)$ were omitted from the output vector.

The coupling of the respiratory system adds an extra parameter to identify, the chest wall elastance, E_{wall}. To identify this parameter, a further model output is required. From Eq. (17), chest wall elastance is directly proportional to thoracic pressure. Fig. 5 illustrates the effect of thoracic pressure on the aortic pressure waveform. The peaks of $P_a(t)$, $P_a(t)_{\max}$, form the outline of $P_{th}(t)$. Thus $\Delta P_{th}(t) \approx \Delta P_a(t)_{\max}$ over one respiratory cycle is a visible condition, and thus $\Delta P_a(t)_{\max}$ can be used to estimate E_{wall}. Therefore, the final output vector employed in this study is defined:

$$X = [\overline{P}_a(t),\ \Delta P_a(t),\ \overline{V}_h(t),\ SV,\ \Delta P_a(t)_{max}] \tag{22}$$

2.6. Parameter estimation

Parameter estimation is performed through iterative adjustment of parameter values from a set of initial conditions to minimise an error function.

2.6.1. Nominal parameters

A nominal parameter estimation or initial values are required. Where possible, parameters were identified using model equations and measurements. Where measurements were unavailable, values from literature were used. A summary of the equations for each parameter is defined in Table 2.

2.6.2. Parameter subset

To ensure practical identifiability [15,23], a common subset of sensitive parameters was chosen for optimisation for all pigs. The parameters E_{wall} and $V_{s,3}$ are crucial for final analyses and were thus automatically included in the final parameter subset. Sensitivity and correlation analyses per the method in [7] identified a common parameter set. The most commonly sensitive parameters from all pigs were then identified and added to the final parameter subset. A common parameter set was required to ensure comparisons between pigs were relevant.

2.6.3. Error function

The error function is a measure of accuracy for identified model outputs. If y^{ref} is a vector containing the N_y reference measurements and $y(p)$ is the output vector of parameter vector, p, each

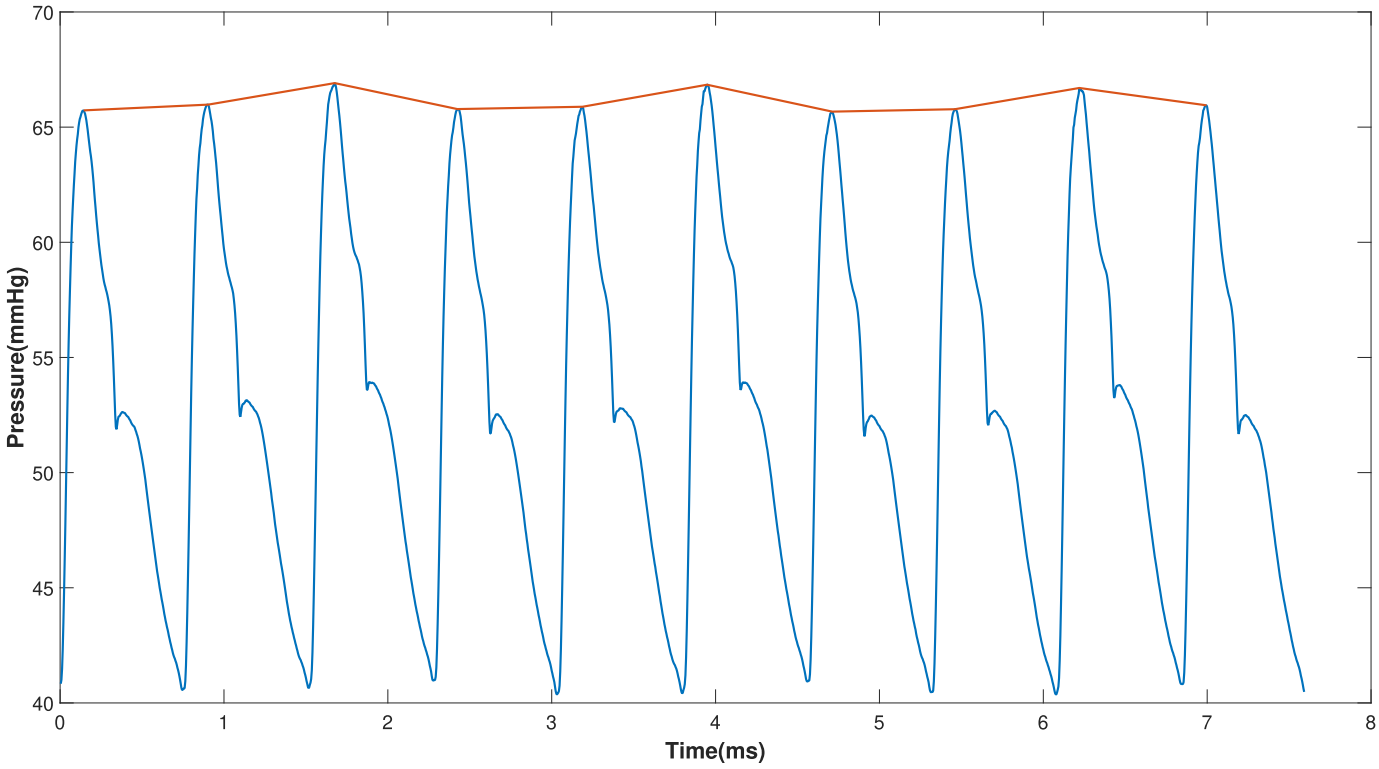

Fig. 5. Effect of thoracic pressure on the aortic pressure waveform. Aortic pressure is shown in blue and thoracic pressure in orange.

Table 2
Parameter definitions.

Parameter	Parameter Definition
E_a	$\frac{\Delta P_a(t)}{CO.T}$ [13]
E_{lv}	$max_T \frac{P_{lv}(t)}{V_{lv}(t)}$ [10]
E_{vc}	$\frac{\Delta P_{vc}(t)}{CO.T}$ [13]
R_c	$\frac{\overline{P}_a(t) - \overline{P}_{vc}(t)}{CO}$ [10]
R_i	0.05mmHg.s/ml [11]
R_o	0.04mmHg.s/ml [11]
$V_{s.3}$	$\overline{V}_{lv}(t) + \frac{\overline{P}_a(t)}{E_a} + \frac{\overline{P}_{vc}(t)}{E_{vc}}$ [10]
E_{wall}	$\frac{E_{rs}}{2}$

output's error is defined as the difference between the measurement and the output:

$$e_i(p) = y_i^{ref} - y_i(p),\ i \in [1, N_y] \tag{23}$$

The error function is then defined using the RMS of all errors:

$$\psi(p) = \sqrt{\frac{\sum_{i=1}^{N_y} e_i(p)^2}{N_y}} \tag{24}$$

2.6.4. Parameter identification

The parameter identification in this work was performed using MATLAB's (The Mathworks, Natick, MA, USA) *fmincon* function. The parameter subset and error function were passed as parameters. Parameter estimation was performed for 4 pigs over 2 preload reduction manoeuvres each.

2.7. Experiment and data

2.7.1. Experimental procedure

The experimental protocol was approved by the Ethics Committee for the use of animals at the University of Liege, Belgium between September - November, 2015 (Reference Number 14–1726). Eight pure Pietrain pigs were anaesthetised and mechanically ventilated. Septic shock was then induced in the subjects via a single infusion of endotoxin (lipopolysaccharide from E. Coli, 0.5 *mg/kg*, infused over 30 *min*). Pre-endotoxin infusion, a 500 *mL* saline solution was administered over 30 *min* simulating fluid resuscitation therapy. Several PEEP driven RMs were performed on each pig both pre- and post- endotoxin. Aortic pressure in the subjects was continually measured via a catheter with a sampling rate of 250 Hz. P_{lv} and V_{lv} were also continually measured at a rate of 250 *Hz* via an admittance pressure volume catheter inserted into the left ventricle via an apical stab.

The airway flow data for Pigs 1 and 5 gave no negative readings, rendering the data unusable for the cardio-pulmonary model. Pigs 2 and 3 both displayed unreliable data with multiple interruptions in the data stream and were thus also unusable for this study. The remaining pigs (Pigs 4, 6, 7 and 8) all had usable data and were used in this work.

2.7.2. Sections of importance

In this study, the section of particular interest was the first RM, as all the following RMs took place post-endotoxin. The presence of endotoxin induced septic shock introduces a multitude of additional physiological mechanisms deemed unsuitable for initial model validation. During the initial RM, PEEP was initially set to $0cm^2H_2O$ and incremented by $5cm^2H_2O$ roughly each minute until a maximum pressure of $20cm^2H_2O$ was reached, with the exception of Pig 7 which had a maximum PEEP of $15cm^2H_2O$. PEEP was then set back to a baseline value of $5cm^2H_2O$.

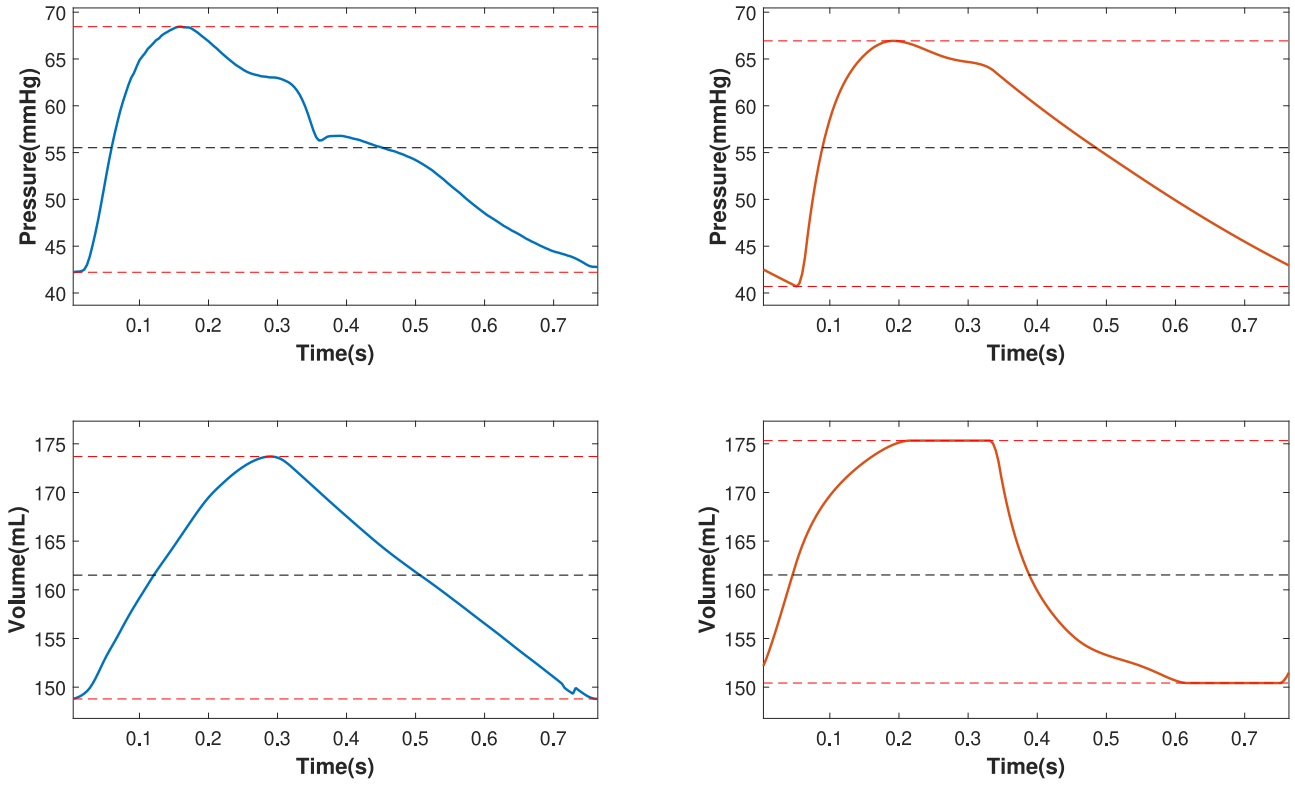

Fig. 6. Identified model waveforms vs measured waveforms. Top left and right show measured and model P_a respectively while bottom left and right show measured and model V_{lv} respectively. Mean values are shown as a dashed black line, and the min and max are shown with dashed red lines.

Sections of data corresponding to each PEEP level of the RM were annotated for all pigs. Parameter estimation was then performed over the first and last five beats of each PEEP section for all pigs.

2.8. Analyses

Model dynamics and quality of fit were analysed by checking the mean absolute error (MAE) of parameter estimates and by comparison of simulated and measured waveforms. Model outputs of the cardio-pulmonary model were compared to outputs of the 3-chamber model to analyse the effects of PEEP on model outputs. The progression of all parameters over the RM were then analysed and compared to expected physiological trends. The effect of thoracic pressure on parameter estimation was analysed by comparing parameter progressions of the two models.

3. Results

3.1. Parameter subset selection

The 2 least sensitive parameters for all pigs were the input and output resistances. They were left out of the final parameter subset. The final parameter subset was defined:

$$P = [E_a,\ E_{lv},\ E_{vc},\ R_c,\ V_{s,3},\ E_{wall}] \tag{25}$$

3.2. Parameter estimation

Parameter estimation was qualified using the MAE of the error vector for each beat. All MAE errors were found to be lower than 0.5%. Parameter estimation was also qualified by plotting simulated waveforms against measurements to ensure model dynamics were accurately captured. Figure 6 shows the comparison of measurement and simulated aortic pressures and left ventricle volumes, displaying their means and ranges. Figure 7 shows the effects of thoracic pressure on both the measured and simulated aortic pressure, illustrating the cardio-pulmonary model's ability to capture the effects of thoracic pressure on the CVS.

3.3. Effect of PEEP on SBV and SV

Figure 8 shows the progression of SBV and SV for both the 3-chamber model and the cardio-pulmonary model. The two models result in almost identical outputs, emphasising the ability of both models to track the left ventricular volume measurements. SV decreases as PEEP is increased, as expected, due to the increased pressure in the thoracic chamber, causing a decrease in venous return and thus a reduction in ventricular preload [26,27]. In healthy patients under normal conditions, SV and SBV are expected to display a strong linear correlation [7]. The relationship between SBV and SV of all pigs is shown in Fig. 9. As expected, the SV and SBV are highly correlated for all pigs displaying a very strong relationship between SBV and SV.

3.4. Effect of PEEP on haemodynamic parameters

Figure 10 shows the progression of parameter estimations of both models over the RM. With the exception of Pig 8, the E_{vc} remains relatively constant over the RM for both models, as expected, since the inherent elastance property of the vessel should not change over the short duration of the RM. Furthermore, as PEEP increases, the estimates of E_{vc} and E_{lv} between the models increasingly diverge. This divergence is expected because the 3-chamber model cannot account for the additional thoracic pressure applied directly to the left ventricle and vena cava.

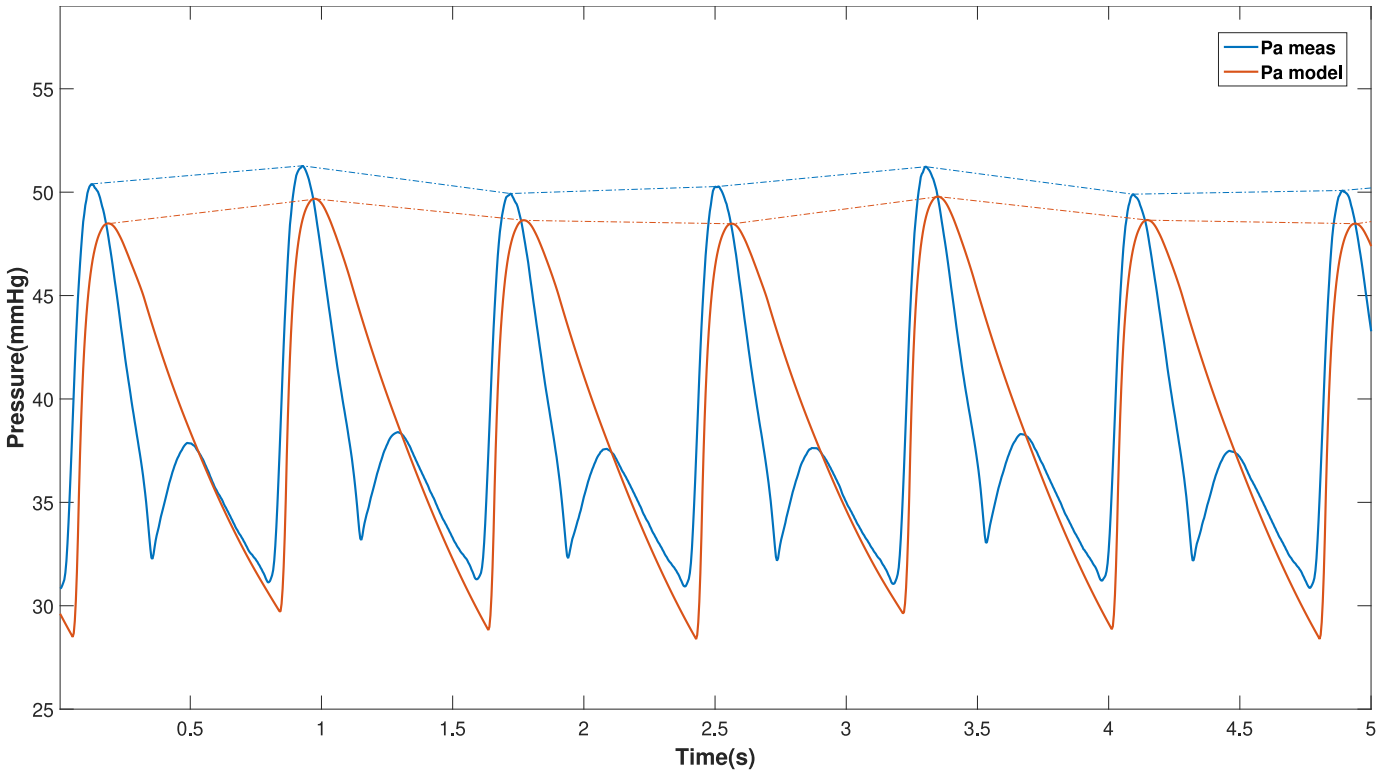

Fig. 7. Modelled waveforms vs measured waveforms. Measured P_a in solid blue and modelled P_a in solid orange. Thoracic pressures are outlined by the dashed lines.

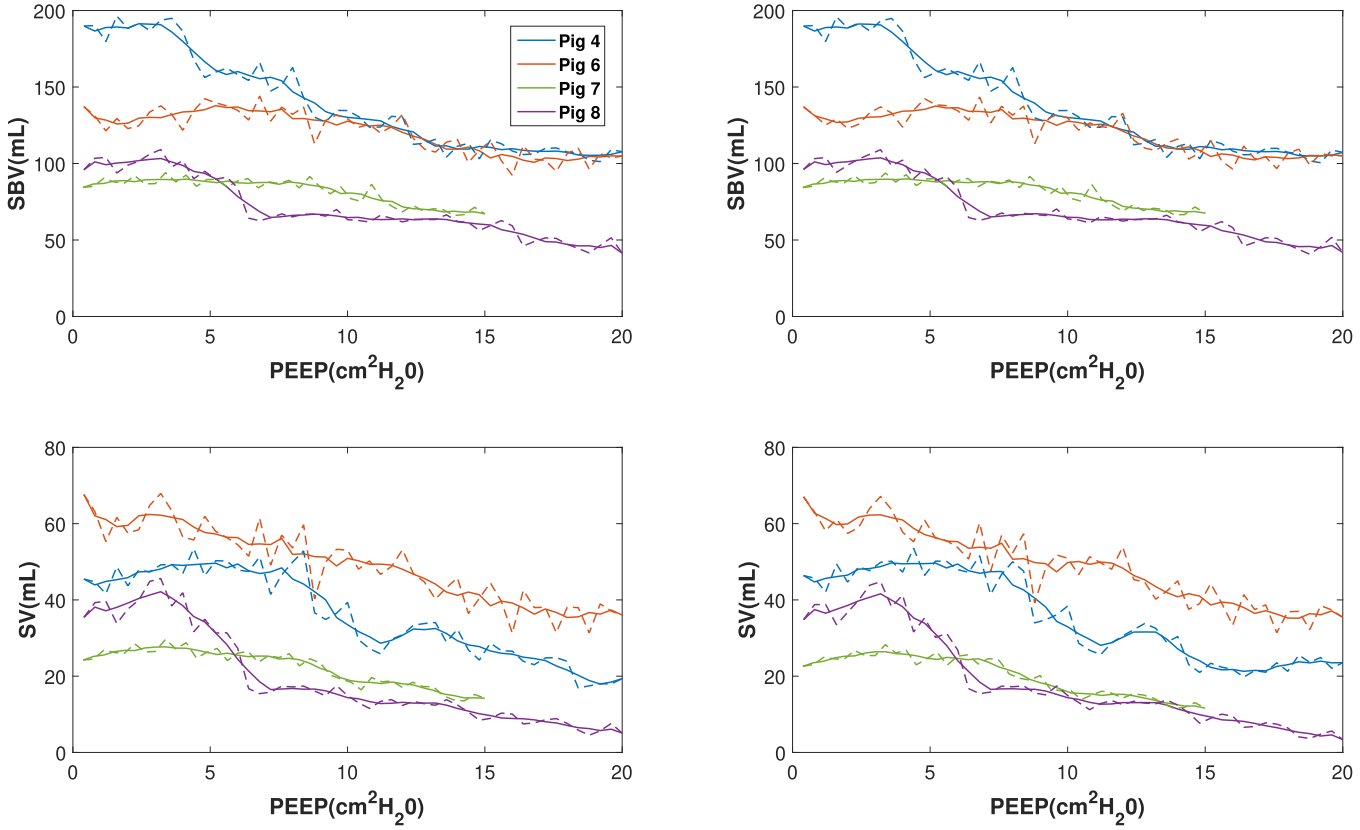

Fig. 8. SV and SBV progression over the RM for both models. Results from the 3 chamber model are shown on the left and results of the cardio-pulmonary model are shown on the right.

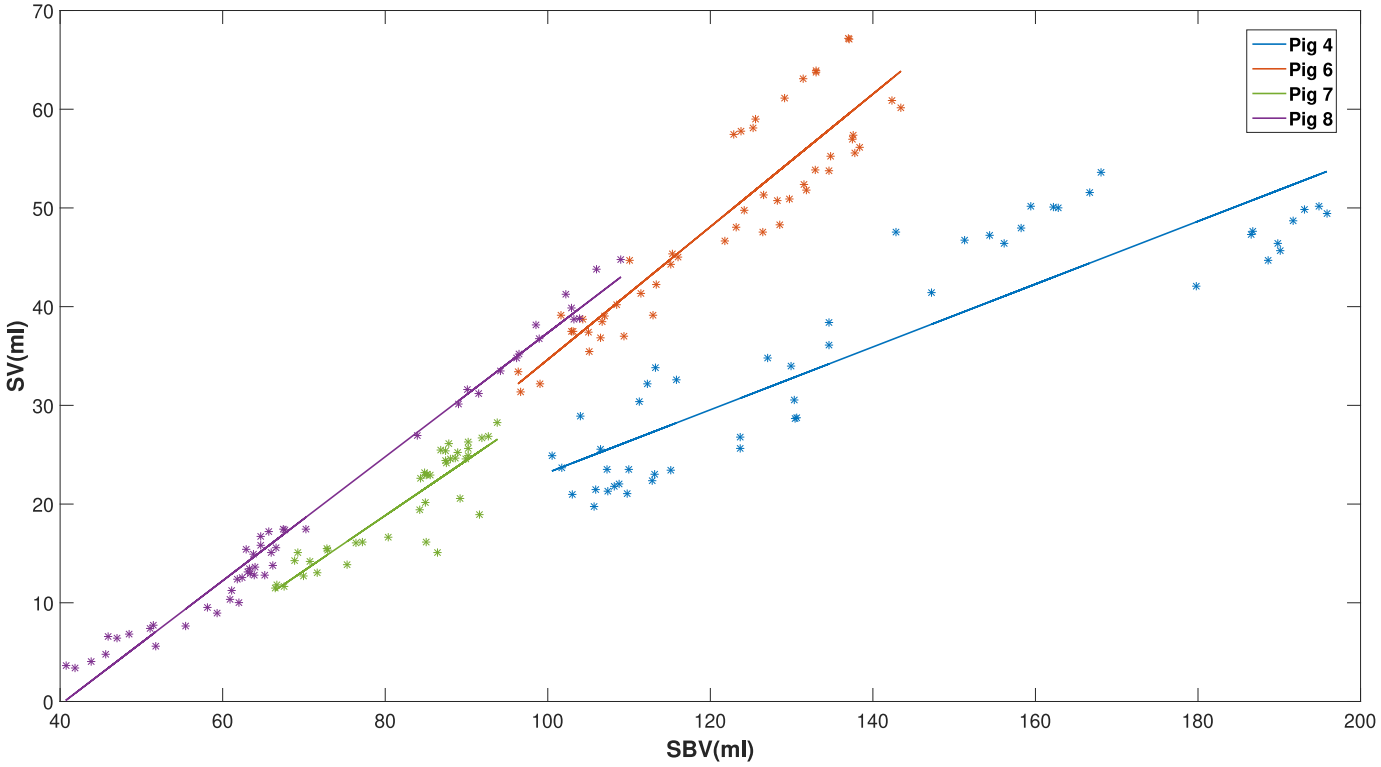

Fig. 9. SBV vs SV for all pigs. Pig 4 is shown in blue, Pig 6 in orange, Pig 7 in green and Pig 8 in purple. Model data are represented by individual points, and the solid lines represent the line of best fit for each pig.

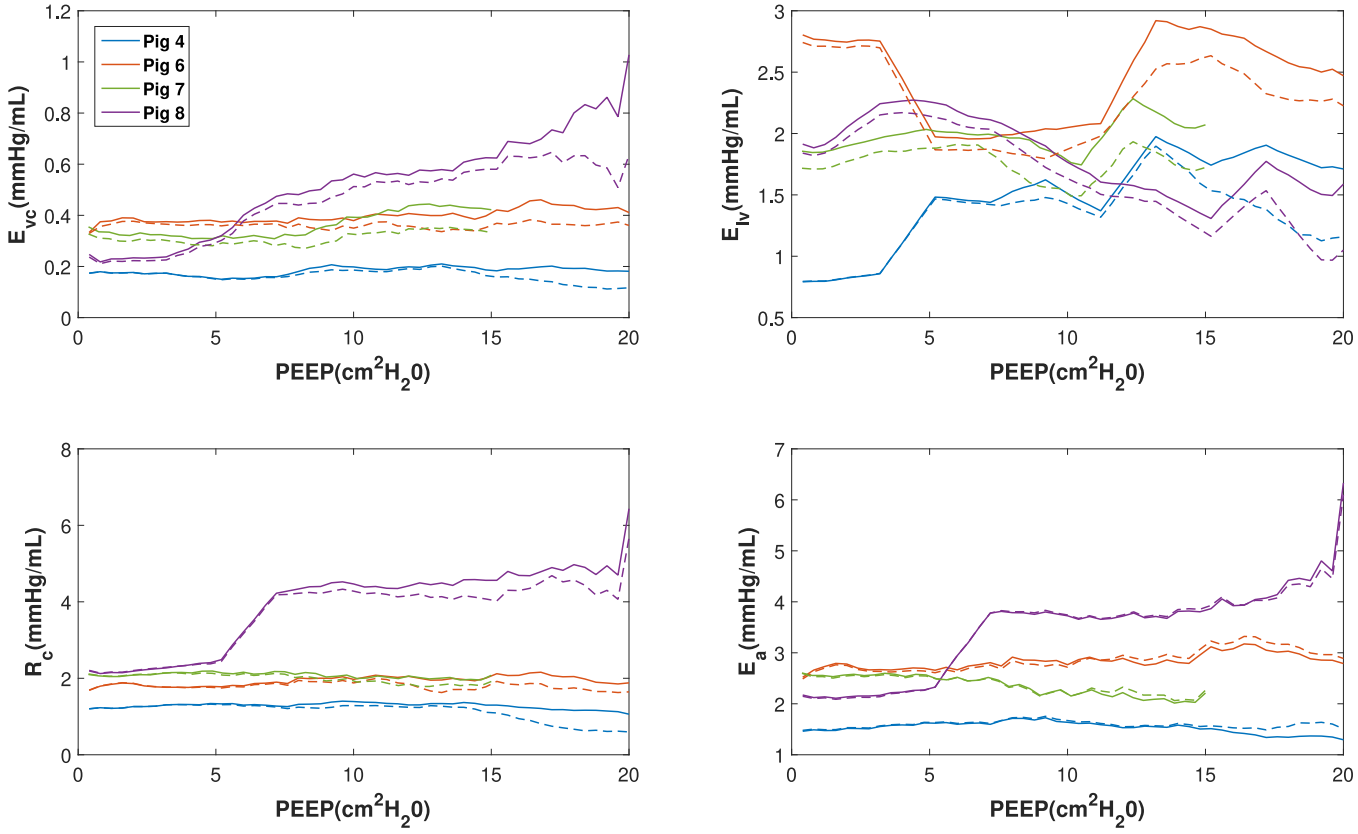

Fig. 10. Parameter estimates over the RM for both models. The dotted line represents cardio-pulmonary estimations and the solid line represents 3-chamber estimations.

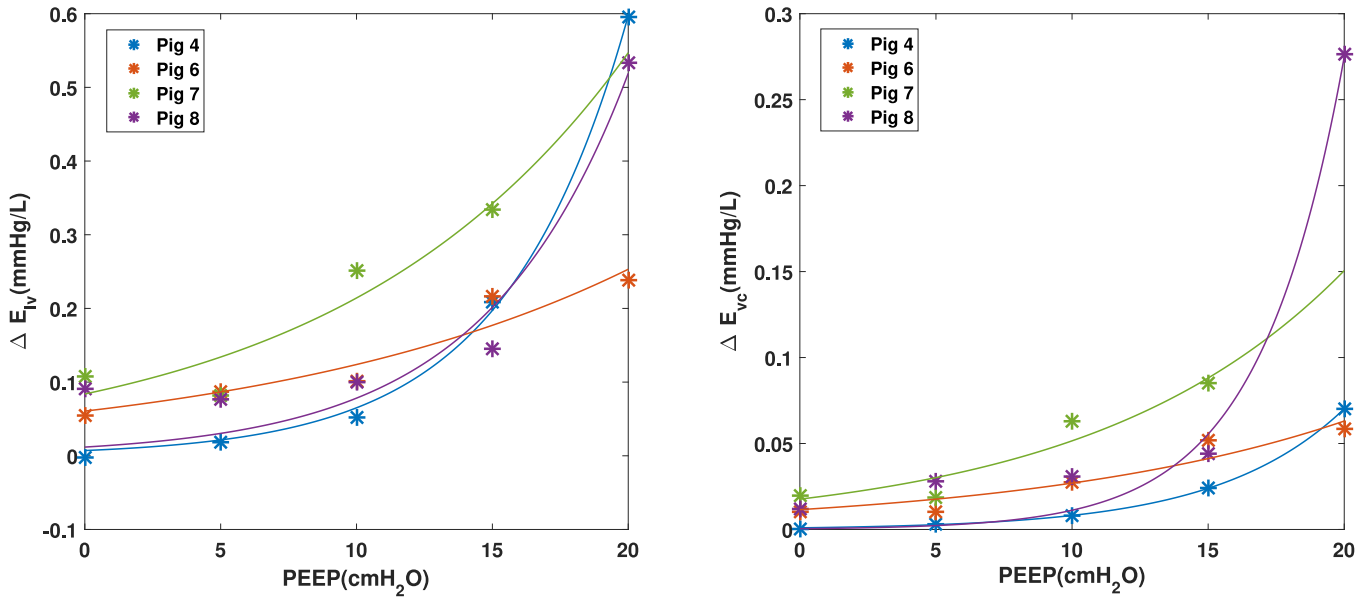

Fig. 11. The difference between elastance estimates from the cardio-pulmonary and 3-chamber models. The left shows identified E_{lv} of the cardio-pulmonary model subtracted from identified E_{lv} of the 3-chamber model for all pigs. The right shows the same for E_{vc}. Actual elastance values (*) are shown against an exponential line of best fit (solid line).

Table 3
r^2 values for exponential fit of elastance divergence.

Pig	r^2 of E_{lv}	r^2 of E_{vc}
4	0.998	0.999
6	0.915	0.906
7	0.889	0.915
8	0.918	0.973

The nature of the divergence is illustrated in Fig. 11. The plot shows identified elastances from the cardio-pulmonary model subtracted from that of the 3-chamber model. The identified elastance from the 3-chamber model are shown to diverge exponentially with increasing PEEP from those of the cardio-pulmonary model. A first order exponential was fitted to the data. The r^2 values for each fit are summarised in Table 3.

R_c and E_a remain relatively constant over the duration of the recruitment manoeuvre for both models. Neither the systemic vasculature nor the aorta are directly affected by ITP and thus large, immediate variations of these parameters with PEEP are not expected. Furthermore, the difference in estimations between the 2 models is much subtler than that of E_{vc} and E_{lv}, further demonstrating the indirect nature of the affect ITP has on these parameters.

4. Discussion

4.1. Comparison of model dynamics

Both models captured the fundamental dynamics of the CVS. Model outputs were validated by assessing the MAE of the parameter estimation and by means of visual inspection to ensure reliable tracking of measurement data. Despite its slight increase in complexity, there was no apparent increase in MAE of the cardio-pulmonary model when compared to the 3-chamber model.

4.2. Model discrepancies

The results shown in Figs. 6-7 do not match measurement volume and pressure waveforms exactly. Despite having near identical means and ranges, the shapes of modelled aortic pressure and left ventricle volume vary slightly from their measured counterparts.

The reason for the discrepancy in volume results from obtaining left ventricular volume via integration of aortic flow. While this produces accurate measurements of SV and mean left ventricular volume used by the error function, it does not provide an accurate overall shape of the left ventricular volume waveform, which would closer resemble the shape of the modelled output.

Similarly, the Dicrotic Notch in the aortic pressure is not present in Fig. 7 as the model definition chosen does not capture this local nonlinear behaviour given its goal is to capture system overall system dynamics and system wide metrics such as stressed blood volume.

4.3. Effect of MV on the CVS

Mechanical ventilation has a wide range of effects on the CVS. It causes an increase in ITP which is directly applied to the heart and the vena cava. As PEEP increases, so too does ITP, and, as such, its effects on the CVS are exacerbated. Increased levels of thoracic pressure are known to inhibit venous return, causing a reduction in preload and ultimately a reduced CO.

As PEEP increased, measured SV decreased significantly, dropping by over 60% in Pigs 4 and 8. Both models were able to successfully track the large variations in SV as PEEP was increased. Furthermore, the models were able to capture the strong relationship between SBV and SV, as shown in Fig. 9, emphasising their ability to accurately estimate SBV and their potential for use in guiding fluid therapy.

E_{vc} remained relatively constant over the RM for 3 of the 4 Pigs. The elastance is an inherent property of the vessel and should not change over small periods of time in healthy subjects. However, Pig 8 showed a large increase in E_{vc}. Pig 8 was diagnosed as being hypovolemic. The model relies on a linear relationship between pressure and stressed blood volume in its passive chambers. Once a subject becomes increasingly hypovolemic, it is possible for the model to enter a non-linear operating range, where estimated parameters are less physiologically relevant or accurate. However, at such low volumes, there is little diagnostic loss as there would

have already been many available signs of such a severe condition, such as very low blood pressure levels.

4.4. Effect of ITP on estimated parameters

The effects of ITP on the CVS can also interfere with a model's ability to produce accurate parameter estimations. In the case of the three chamber model, which is unable to account for thoracic pressure, the model is unable to separate thoracic pressure from simulated left ventricle pressure and venous pressure. Thus, while some parameters remain unaffected, some parameters show large deviations compared to the cardio-pulmonary model.

As expected, estimations of SBV and aortic elastance remained unaffected by thoracic pressure. Since blood flow through the system remains the same for both models, it can be deduced SBV would remain the same as well, since stressed blood volume is the integral of blood flow in the system. If SBV in the aortic chamber remains constant, from Eq. (1), any change in pressure results in a direct change in elastance and vice versa. Since modelled aortic pressure is not directly affected by thoracic pressure and the stressed volume in the aortic chamber remains constant, it can be deduced aortic elastance estimates between the 2 models should not change either.

As shown in Fig. 10, both the left ventricle and vena cava elastance estimates of the two models diverged as PEEP increased. The divergence was found to be exponential with PEEP, as illustrated by Fig. 11. This outcome is expected because unlike aortic pressure, both the left ventricle pressure and vena cava pressure are directly affected by thoracic pressure. Measured pressures are comprised of pressure caused by stressed volume in the chamber and the thoracic pressure caused by MV. Since the three chamber model is unable to account for thoracic pressure, it assumes pressure measurements are caused exclusively by SBV. This necessary assumption due to the model's definition results in elastance estimations which increase directly with PEEP. Since the cardiopulmonary model is able to distinguish between thoracic pressure and pressure caused by SBV, it produces a more physiologically accurate estimation of elastance, one which does not fluctuate with PEEP.

4.5. Limitations

4.5.1. Simplicity of model

One of the biggest limitations of the model presented in this work is the omission of the pulmonary circulation [10,28]. Indeed, it is assumed the systemic and pulmonary circulations can be treated independently for assessing SBV, which is not physiologically accurate. Furthermore, under normal operating conditions, the heart experiences ventricular interactions due to the heart being enclosed in a fibrous membrane called the pericardium. The physiological connection between left and right ventricles causes a compressive force applied to the left ventricle when the right undergoes filling. With only one circulation being considered this interaction cannot be accounted for, though it is typically small except in pulmonary embolism [29,30]. Equally, the model's simplicity ensures identifiability and is still able to capture observed dynamics.

Another limitation of the model is the absence of the left atrium. At the end of filling, the left atrium contracts to provide an additional amount of blood to the ventricle. It has not yet been shown the time varying elastance theory can be applied to the atria as it is done to the ventricle. Other authors have developed alternate methods to represent the atria such as the multi-scale model [28]. However, these models use large numbers of parameters, rendering the model structurally unidentifiable due to the limited data clinically available.

A further limitation of the model is the fixing of the input resistance for parameter estimation. Several studies have cited raising PEEP increases the resistance to venous return, which is linked to reduced ventricular preload and thus reduced SV. With the resistance to venous return fixed for parameter estimation, the model accounts for this in other ways which means some identified parameters may not be entirely physiologically accurate. However, it is not immediately evident to what degree estimations are affected. Sensitivity analyses performed in this study and several others [7,8,13] found input resistance to be the least sensitive parameter in the parameter estimation process, implying that it has very little effect on overall system dynamics compared to other parameters. Furthermore, the model is still able to accurately capture expected trends of haemodynamic parameters. Parameter trends are arguably of much greater importance as they are more clinically relevant in assessing a patient's response to treatment than exact parameter values, which have less physiological importance given the wide variation of parameter values among individuals.

4.5.2. Experimental data

The study was limited by the small sample size of experimental data available. Furthermore, of the 8 pigs which underwent the experimental procedures, only 4 produced suitable measurement data for use in this study. Despite the small sample size, the porcine data used in this study provided accurate information to run and validate the model, including left ventricle volume, which is not typically available in the ICU. Such animal studies are intensive, time consuming, and costly, thus only few experiments are performed. However, the quality of data available for validation is very high, and unavailable in human subjects. Thus, this study and data provide a foundation of work, which can be confidently built on to investigate trends in a larger population of human subjects, while directing it towards a clinical setting.

5. Conclusions

The work in this paper investigated the novel cardio-pulmonary model and its ability to reproduce cardiovascular system dynamics and physiologically expected trends over the course of a preload reduction manoeuvre. It proved successful in reproducing overall CVS dynamics and importantly, the effects of ITP on the CVS without skewing other model parameters.

The model outputs and estimated parameters were also compared to the original 3 chamber model from which the cardiopulmonary model was derived. Despite the increase in model complexity, there was no loss in the model's ability to accurately estimate haemodynamic parameters and reproduce system dynamics. Furthermore, the cardio-pulmonary model was able to demonstrate how MV affected parameter estimations as PEEP was increased. The 3 chamber model was shown to produce parameter estimations which fluctuated directly with PEEP, while the cardiopulmonary model estimations remained more stable, suggesting its ability to produce more physiologically accurate parameter estimations under higher PEEP conditions.

Ethics approval

The experimental protocol was approved by the Ethics Committee for the use of animals at the University of Liege, Belgium between September - November, 2015 (Reference Number 14–1726).

Declaration of Competing Interest

The authors declare no financial or other conflicts of interest.

References

[1] J.L. Knopp, J.G. Chase, K.T. Kim, G.M. Shaw, Model-based estimation of negative inspiratory driving pressure in patients receiving invasive NAVA mechanical ventilation, Comput. Methods Programs Biomed. 208 (2021), doi:10.1016/j.cmpb.2021.106300.

[2] A.C. Guyton, J.E. Hall, Medical Physiology, 11th ed. Jackson, MS: Elsevier Saunders, 2006.

[3] A.Y. Denault, J. Gorcsan, M.R. Pinsky, Dynamic effects of positive-pressure ventilation on canine left ventricular pressure-volume relations, J. Appl. Physiol. 91 (1) (2001) 298–308, doi:10.1152/jappl.2001.91.1.298.

[4] S. Schuster, R. Erbel, L.S. Weilemann, W. Lu, B. Henkel, S. Wellek, H. Schinzel, J. Meyer, Hemodynamics during PEEP ventilation in patients with severe left ventricular failure studied by transesophageal echocardiography, Chest 97 (5) (1990) 1181–1189, doi:10.1378/chest.97.5.1181.

[5] J.J. Maas, M.R. Pinsky, L.P. Aarts, J.R. Jansen, Bedside assessment of total systemic vascular compliance, stressed volume, and cardiac function curves in intensive care unit patients, Anesth. Analg. 115 (4) (2012) 880–887, doi:10.1213/ANE.0b013e31825fb01d.

[6] D.A. Reuter, A. Kirchner, T.W. Felbinger, F. C. Weis, E. Kilger, P. Lamm, A.E. Goetz, Usefulness of left ventricular stroke volume variation to assess fluid responsiveness in patients with reduced cardiac function, Crit. Care Med. 31 (5) (2003) 1399–1404.

[7] A. Pironet, Model-Based prediction of the response to vascular filling therapy, University of Liège, Belgium, 2016 phd dissertation.

[8] A. Pironet, T. Desaive, J.G. Chase, P. Morimont, P.C. Dauby, Model-based computation of total stressed blood volume from a preload reduction experiment, IFAC Proc. Vol. 47 (3) (2014) 5641–5646, doi:10.3182/20140824-6-ZA-1003.00548.

[9] L. Murphy, S. Davidson, J.G. Chase, J.L. Knopp, T. Zhou, T. Desaive, Patient-specific monitoring and trend analysis of model-based markers of fluid responsiveness in sepsis: a proof-of-concept animal study, Ann. Biomed. Eng. 48 (2020) 682–694.

[10] A. Pironet, P.C. Dauby, J.G. Chase, S. Kamoi, N. Janssen, P. Morimont, B. Lambermont, T. Desaive, Model-based stressed blood volume is an index of fluid responsiveness, IFAC Pap. Online 48 (20) (2015) 291–296, doi:10.1016/j.ifacol.2015.10.154.

[11] J.A. Revie, D.J. Stevenson, J.G. Chase, C.E. Hann, B.C. Lambermont, A. Ghuysen, P. Kolh, G.M. Shaw, S. Heldmann, T. Desaive, Validation of subject-specific cardiovascular system models from porcine measurements, Comput. Methods Programs Biomed. 109 (2) (2013) 197–210, doi:10.1016/j.cmpb.2011.10.013.

[12] T. Desaive, O. Horikawa, J.P. Ortiz, J.G. Chase, Model-based management of cardiovascular failure: where medicine and control systems converge, Annu. Rev. Control 48 (2019) 383–391.

[13] S. de Bournonville, A. Pironet, C. Pretty, J.G. Chase, T. Desaive, Parameter estimation in a minimal model of cardio-pulmonary interactions, Math Biosci. 313 (2019) 81–94, doi:10.1016/j.mbs.2019.05.003.

[14] S. Davidson, D.O. Kannangara, C.G. Pretty, S. Kamoi, T. Desaive, J.G. Chase, A novel approach for deriving a patient specific beat-to-beat estimate of the cardiac driver function, IFAC Pap. Online 48 (20) (2015) 348–353, doi:10.1016/j.ifacol.2015.10.164.

[15] A. Pironet, P.D. Docherty, P.C. Dauby, J.G. Chase, T. Desaive, Practical identifiability analysis of a minimal cardiovascular system model, Comput. Methods Programs Biomed. 171 (2019) 53–65, doi:10.1016/j.cmpb.2017.01.005.

[16] J.G. Chase, J.C. Preiser, J.L. Dickson, A. Pironet, Y.S. Chiew, C.G. Pretty, G.M. Shaw, B. Benyo, K. Moeller, S. Safaei, M. Tawhai, Next-generation, personalised, model-based critical care medicine: a state-of-the art review of in silico virtual patient models, methods, and cohorts, and how to validation them, Biomed Eng. Online 17 (1) (2018) 1–29.

[17] Y.S. Chiew, J.G. Chase, G.M. Shaw, A. Sundaresan, T. Desaive, Model-based peep optimisation in mechanical ventilation, Biomed. Eng. Online 10 (2011) 111, doi:10.1186/1475-925X-10-111.

[18] A. Sundaresan, J.G. Chase, G.M. Shaw, Y.S. Chiew, T. Desaive, Model-based optimal PEEP in mechanically ventilated ARDS patients in the intensive care unit, Biomed. Eng. Online 10 (2011) 64, doi:10.1186/1475-925X-10-64.

[19] J.H.T. Bates, Lung Mechanics: An Inverse Modeling Approach, Cambridge University Press, 2009.

[20] A. Baydur, Monitoring lung mechanics, Chestn 121 (2) (2002) 324–326, doi:10.1378/chest.121.2.324.

[21] S.E. Morton, J.L. Knopp, J.G. Chase, P. Docherty, S.L. Howe, K. Möller, G.M. Shaw, M. Tawhai, Optimising mechanical ventilation through model-based methods and automation, Annu. Rev. Control 48 (2019) 369–382, doi:10.1016/j.arcontrol.2019.05.001.

[22] Y.S. Chiew, J.G. Chase, B. Lambermont, N. Janssen, C. Schranz, K. Moeller, G.M. Shaw, T. Desaive, Physiological relevance and performance of a minimal lung model: an experimental study in healthy and acute respiratory distress syndrome model piglets, BMC Pulm. Med. 12 (59) (2012), doi:10.1186/1471-2466-12-59.

[23] A. Pironet, P.C. Dauby, J.G. Chase, P.D. Docherty, J.A. Revie, T. Desaive, Structural identifiability analysis of a cardiovascular system model, Med. Eng. Phys. 38 (5) (2016) 433–441, doi:10.1016/j.medengphy.2016.02.005.

[24] S. Audoly, L. D'Angio, M.P. Saccomani, C. Cobelli, Global identifiability of linear compartmental models, IEEE Trans. Biomed. Eng. 45 (1) (1998) 36–47.

[25] S. Audoly, G. Bellu, L. D'Angio, M.P. Saccomani, C. Cobelli, Global identifiability of nonlinear models of biological systems, IEEE Trans. Biomed. Eng. 48 (1) (2001) 55–65.

[26] N. Soni, P. Williams, Positive pressure ventilation: what is the real cost? Br. J. Anaesth. 101 (4) (2008) 446–457, doi:10.1093/bja/aen240.

[27] C. Starfinger, J.G. Chase, C.E. Hann, G. M. Shaw, P. Lambert, B.W. Smith, E. Sloth, A. Larsson, S. Andreassen, S. Rees, Model-based identification of PEEP titrations during different volemic levels, Comput. Methods Programs Biomed. 91 (2) (2008) 135–144, doi:10.1016/j.cmpb.2008.03.005.

[28] A. Pironet, P.C. Dauby, S. Paeme, S. Kosta, J.G. Chase, T. Desaive, Simulation of left atrial function using a multi-scale model of the cardiovascular system, PLoS ONE 8 (6) (2013) E65146, doi:10.1371/journal.pone.0065146.

[29] B.W. Smith, J.G. Chase, R.I. Nokes, G.M. Shaw, T. David, Velocity profile method for time varying resistance in minimal cardiovascular system models, Phys. Med. Biol. 48 (20) (2003) 3375, doi:10.1088/0031-9155/48/20/008/meta.

[30] C. Starfinger, C.E. Hann, J.G. Chase, T. Desaive, A. Ghuysen, G.M. Shaw, Model-based cardiac diagnosis of pulmonary embolism, Comput. Methods Programs Biomed. 87 (1) (2007) 46–60, doi:10.1016/j.cmpb.2007.03.010.